Published in final edited form as:
Neuroscience. 2008 June 2; 153(4): 1390–1401. doi:10.1016/j.neuroscience.2008.02.034.

Inspiratory-phase Short Time Scale Synchrony in the Brainstem Slice is Generated Downstream of the PreBötzinger Complex

Joy Y. Sebe and **Albert J. Berger**
Graduate Program in Neurobiology and Behavior, Department of Physiology and Biophysics, University of Washington School of Medicine, Seattle WA 98195

Abstract

Respiratory neurons are synchronized on a long time scale to generate inspiratory and expiratory-phase activities that are critical for respiration. Long time scale synchrony within the respiratory network occurs on a time scale of more than hundreds of milliseconds to seconds. During inspiration, neurons are synchronized on a short time scale to produce synchronous oscillations, which shape the pattern of inspiratory motor output. This latter form of synchrony within the respiratory network spans a shorter time range of tens of milliseconds. In the neonatal mouse rhythmically active medullary slice preparation, we recorded bilateral inspiratory activity from hypoglossal (XII) rootlets to study where in the slice synchronous oscillations are generated. Based on previous work that proposed the origin of these oscillations, we tested the PreBötzinger Complex (PreBötC) and the XII motor nucleus. Unilateral excitation of the PreBötC, via local application of a perfusate containing high K^+, increased mean inspiratory burst frequency bilaterally (296 ± 66%; n=10, $p<0.01$), but had no effect on the relative power of oscillations. In contrast, unilateral excitation of the XII nucleus increased both mean peak integrated activity bilaterally (ipsilateral: 41 ± 10%, $p<0.01$;contralateral: 17 ± 7%; $p<0.05$, n=10) and oscillation power in the ipsilateral (50 ± 17%, n=7, $p<0.05$), but not in the contralateral rootlet. Crosscorrelation analysis of control inspiratory activity recorded from the left and right XII rootlets produced crosscorrelation histograms with significant peaks centered around a time lag of zero and showed no subsidiary harmonic peaks. Coherence analysis of left and right XII rootlet recordings demonstrated that oscillations are only weakly coherent. Together, the findings from local application experiments and crosscorrelation and coherence analyses indicate that short time scale synchronous oscillations recorded in the slice are likely generated in or immediately upstream of the XII motor nucleus.

Keywords

oscillations; hypoglossal; premotor; power spectrum; crosscorrelation; coherence

Synchronous oscillations of brain activity have been described almost ubiquitously in the mammalian brain and the frequency of these span a wide range of time scales. Synchrony on a millisecond time scale, which generates 2–100 Hz oscillations, has been implicated in many

Corresponding Author: Joy Y. Sebe, Department of Neurological Surgery, University of California, San Francisco, 533 Parnassus Ave. Room U-240, Box 0520, San Francisco, CA 94113, joysebe@gmail.com, Tel: (415) 502-1026, Fax: (415) 353-3937.
Section Editor: Dr. Minoru Kimura

functions, such as memory (Kahana,2006) and sensory processing (Stopfer et al.,1997; Gelperin,2006), sleep (Steriade et al.,1993) and movement (Baker and Baker,2003).

Inspiratory motoneurons within the brainstem respiratory network are synchronized on long and short time scales to generate inspiratory rhythm and inspiratory-phase short time scale synchronous oscillations, respectively. On a long time scale (more than hundreds of milliseconds), PreBötzinger Complex (PreBötC) neurons located in the medulla generate inspiratory rhythm (Smith et al.,1991; Koshiya and Guyenet,1996; Pierrefiche et al.,1998; Johnson et al.,2001) that is characterized by regularly recurring bursts of action potentials, or inspiratory bursts, each of which are followed by a period of quiescence. Inspiratory rhythm results in contractions in inspiratory muscles and is critical for respiration. Inspiratory neurons are further synchronized on a short time scale (tens of milliseconds) to generate synchronous oscillations in motoneuron firing during an inspiratory burst (Cohen et al.,1997; Funk and Parkis,2002). Inspiratory-phase short time scale synchronous oscillations are characterized by clusters of action potentials that occur at a regular interval and are separated by periods of little or no spike firing.

The function of inspiratory-phase synchronous oscillations in the brainstem has been investigated, although to a lesser extent relative to oscillations observed in other brain regions (Seager et al.,2002). Short time scale synchronous oscillations are not required for respiratory rhythm generation, but they are important in shaping the pattern of inspiratory discharge. At the motoneuron level, oscillations increase the input-output efficiency of inspiratory motoneurons as well as the precision of spike timing (Parkis et al.,2003). Furthermore, synchronous firing of inspiratory motoneurons may also serve to increase muscle force output (Baker et al.,1999).

Since Cohen initiated an extensive study of these oscillations in 1973 (Cohen,1973), the origin of short time scale synchronous oscillations has been the subject of great interest. These oscillations have been categorized into high frequency and medium frequency oscillations (HFOs and MFOs, respectively). Although HFOs and MFOs typically occur at high and low frequencies, respectively, the frequency ranges in which these oscillations occur are not exclusively their defining characteristic. Instead, the characteristics that distinguish HFOs from MFOs reflect the different regions of the inspiratory network in which they are thought to be generated.

Short time scale synchronous oscillations recorded from different motor pools or from the left and right phrenic nerves are considered HFOs if they are temporally coincident and occur at the same frequency. In order for oscillations recorded from different motor pools or from the left and right phrenic nerves to be synchronized in this way, they must be generated by a common input source, such as the inspiratory pattern generator (Cohen et al.,1997), that transmits inspiratory activity to multiple motor pools. Within the slice, this common input source corresponds to the PreBötC, which generates and transmits inspiratory rhythm to hypoglossal motoneurons (HMs) (Smith et al.,1991).

In contrast, if short time scale synchronous oscillations recorded from different motor pools or from the left and right phrenic nerves are not temporally correlated and do not occur at the same frequency they are considered MFOs. Given that MFOs exhibited by different motor outputs are asynchronous, they are likely generated within or immediately upstream of the motor pool (Cohen et al.,1987; Christakos et al.,1991; Cohen et al.,1997). Thus, within the slice preparation, MFOs would likely be generated by upstream premotoneurons that send projections to the XII nucleus or within the XII nucleus itself.

Although the regions of the inspiratory network in which short time scale synchronous oscillations (MFOs and HFOs) may be generated have been proposed (Christakos et al.,

1991; Cohen et al.,1997), only one lesion study in the cat brainstem has addressed where oscillations may be generated (Richardson and Mitchell,1982). In the present work, we have taken advantage of the simplified respiratory network within the rhythmically active medullary slice preparation to determine where in the slice synchronous oscillations may be produced. Within the rhythmic slice, oscillations may be produced in the PreBötC, which generates inspiratory rhythm, by subsequent premotoneurons that project to HMs or within the XII motor nucleus itself. We tested these candidate regions using a combination of experimental and data analysis techniques.

To experimentally test where in the slice short time scale synchronous oscillations are generated, we unilaterally excited either the PreBötC or the XII nucleus and monitored changes in the power spectral density whose shape is dependent on the degree to which synchronous oscillations occur in inspiratory-phase XII nerve activity. From intracellular recordings of rhythmically active phrenic motoneurons, we know that inspiratory motoneurons receive inspiratory-phase oscillatory synaptic inputs that increase spike firing probability and that action potentials occur at the peaks of the oscillatory inputs (Parkis et al.,2003). In the present work, we have increased the excitability of neurons in the PreBötC or the XII nucleus. If oscillations are generated in the PreBötC, PreBötC neurons should receive oscillatory synaptic inputs from other PreBötC neurons. Unilaterally exciting PreBötC neurons should increase the probability that these neurons will fire action potentials at the peaks of the oscillatory synaptic inputs thereby increasing oscillation power. If instead oscillations are generated in the XII nucleus or immediately upstream in the premotor area, HMs should receive oscillatory synaptic inputs from neurons within the XII nucleus or from premotoneurons. Thus if oscillations have a motor or premotor origin, unilaterally exciting either the XII nucleus, and not the PreBötC, should increase the probability that HMs will fire at the peaks of the oscillatory synaptic inputs and thereby this should increase oscillation power.

We also applied crosscorrelation and coherence analyses to determine whether short time scale synchronous oscillations recorded from the left and right XII rootlets are temporally coincident and occur at the same frequency, respectively. If bilaterally recorded oscillations are temporally coincident and occur at the same frequency, then the oscillations would likely be generated by the PreBötC since this structure serves as the common input source within the slice. In contrast, if bilaterally recorded oscillations are not temporally coincident and do not occur at the same frequency, they are likely to be generated individually within the XII nucleus or by premotoneurons that project to HMs.

Experimental procedures

Slice Preparation

In vitro experiments were performed on the rhythmically active medullary slice preparation from Swiss-Webster mice (P4-7). Mice were anesthetized with isoflurane and sacrificed by decapitation in accordance with the regulations of the University of Washington Institutional Animal Care and Use Committee (IACUC).

Methods used in dissecting the rhythmically active medullary slice preparation have been described previously (Funk et al.,1993; Sebe et al.,2006). In brief, the medulla and cervical spinal cord were isolated and removed from the mouse. The brainstem and spinal cord were pinned onto a Sylgard®® block and the block was mounted into a vibratome platform (Pelco 101 Series 1000, Redding, CA). Brainstem slices were then cut from rostral to caudal. After the facial nucleus was no longer visible, another 200 μm slice was cut prior to cutting the rhythmic slice. The thickness of the rhythmic slice was increased from 500–700 μm depending on the age of mouse. Slices from younger mice were thinner than those obtained from older mice. Slices were placed into the recording chamber and superfused for at least 20 minutes

with 8 mM K^+ artificial cerebrospinal fluid (ACSF) before recording began. Throughout the dissection and the experiment, the ACSF was continuously bubbled with a 95% O_2 and 5% CO_2 gas mixture.

Recording

For the rhythmically active slice preparation, the temperature of the custom-made recording chamber was maintained between 27 and 28°C. Glass suction electrodes were pulled from borosilicate glass and filled with ACSF to record from the cut ends of XII rootlets. Raw nerve signals were sampled at 5 kHz, amplified, and bandpass filtered (0.1 Hz – 2 kHz) using CyberAmp 320 and pClamp8 (Axon Instruments, Union City, CA). To measure integrated nerve activity, the filtered signal was rectified and integrated using a custom built "leaky" integrator with a time constant of 100 ms.

Solutions

The normal ACSF used for rhythmically active slice preparations contained (in mM): 118 NaCl, 3 KCl, 1 $MgCl_2$, 1 NaH_2PO_4, 25 $NaHCO_3$, 30 D-glucose and 1.5 $CaCl_2$. The osmolarity of the ACSF was 300 mOsm and the ACSF was pH adjusted to 7.4 with NaOH. For recording spontaneous rhythmic activity, the same ACSF was used except that KCl concentration was elevated to 8 mM KCl. ACSF was superfused over the preparation at 2–3 ml/min and recycled using a peristaltic pump (Rainin). For local perfusion, ACSF within the perfusion pipette contained fast green (11.2mg/100ml) or fast green plus varying concentrations of K^+ (8, 20, 60 or 80 mM).

Local Perfusion

In numerous preliminary experiments, the PreBötC was located using a combination of ventrolateral landmarks (i.e. inferior olive and nucleus ambiguus) and field electrode recordings of inspiratory activity in the PreBötC. Knowledge acquired from these preliminary experiments regarding the location of the PreBötC with respect to ventrolateral landmarks was used to subsequently target the PreBötC for local perfusion. For unilateral excitation of the XII nucleus, the XII nucleus and its borders were easily visualized in the slice. The local perfusate was delivered in the direction parallel to the flow path of the bath perfusate. To do this, a local perfusion pipette was placed just above the surface of the slice and at the upstream border of the target region (PreBötC or XII nucleus). During local perfusion, the local perfusate was rapidly removed using an uptake pipette that was placed downstream of and within 0.5 mm of the local perfusion pipette. The local uptake pipette was positioned so that the local perfusate was limited to the target region. To visualize the spread of the local perfusate, fast green was included in all locally perfused ACSF solutions. Control experiments demonstrated that local perfusion of fast green alone had no effect on inspiratory-phase activity and synchronous oscillations (data not shown, n=3). We documented the region onto which the perfusate was applied by capturing a digital image of the spread of fast green during the experiment (Figure 1). Due to the anatomy of the rhythmic slice, the slice needed to be either positioned with the rostral or caudal (Figure 1) side up to expose and perfuse the PreBötC or XII nucleus, respectively. In order to locally perfuse the PreBötC and, subsequently, the XII nucleus in the same rhythmic slice, the XII rootlets would have had to be expelled from suction electrodes and the slice flipped over. This procedure stretches the rootlets thereby significantly reducing the signal to noise ratio (data not shown). Therefore, for each rhythmic slice the local perfusate was unilaterally applied either only to the PreBötC or to the XII nucleus, but not to both.

In all experiments, the local perfusion pipette initially contained ACSF with 8 mM K^+. This K^+ concentration was then raised to 60 or 80 mM for the PreBötC experiments and to 20 mM for the XII nucleus experiments. These elevated K^+ concentrations in the local perfusates were experimentally determined to increase slice excitability. For unilateral perfusion of the

PreBötC, 60 mM K^+ was the lowest concentration tested (30, 40, 60 and 80 mM) that had an effect on inspiratory activity. With respect to the XII nucleus, 20 mM K^+ was the lowest concentration tested (30, 40, 60 and 80 mM) that elicited an effect on inspiratory activity. K^+ concentrations greater than 30 mM, when applied to the XII nucleus, induced high levels of tonic activity in the XII rootlet recording that masked the inspiratory bursts. However, when inspiratory bursts could be distinguished from the tonic activity, we observed no change in inspiratory burst frequency following unilateral local perfusion of high K^+ onto the XII nucleus (data not shown). We switched between perfusate solutions using a locally built valve box that controlled which solution passed through a miniature manifold connected to the local perfusion pipette. The time at which the solution was switched was digitally recorded using a voltage output from the valve box that was sent to the AD converter. To minimize dead space in the perfusion pipette, perfusate was delivered from the manifold to the tip of the pipette via quartz capillary tubing. In all experiments, an increase in XII rootlet activity (PreBötC perfusion: increase in inspiratory burst frequency, XII nucleus perfusion: increase in peak integrated activity) occurred within 3 minutes following the switch to a perfusate containing elevated K^+. During local perfusion, elevated XII rootlet activity achieved a steady state level in all experiments. For PreBötC and XII nucleus perfusions, this steady state level of activity was characterized by a constant elevated inspiratory burst frequency and peak integrated activity, respectively.

Data Analysis

To analyze XII rootlet activity in the control condition, we selected consecutive inspiratory bursts that occurred just before the switch to a perfusate containing high K^+. To assess changes in XII rootlet activity during local perfusion of high K^+, we selected the first inspiratory burst that marked the onset of steady state activity and consecutive inspiratory bursts thereafter. Individual inspiratory bursts were selected in Clampfit (Axon Instruments) and analyzed in Igor Pro (Wavemetrics, Inc) using routines developed by Dr. Randy K. Powers. For each recording condition, 7–18 inspiratory bursts were used to create 7–18 absolute power spectra in which the frequency resolution was 1–2 Hz. Average absolute power spectra were computed by averaging the 7–18 absolute power spectra for each condition. Average relative power spectra were calculated from the average absolute power spectra by dividing the absolute power at each data point (0–99 Hz) by the absolute power for all data points (0–99 Hz). Average relative and absolute power spectra were used to compute changes in the relative power of oscillations and in the coherence between left and right XII rootlet activity, respectively.

To measure the relative power of short time scale synchronous oscillations, we located the dominant peaks in the average relative power spectra computed from inspiratory bursts recorded in the control condition and following local perfusion of high K^+. For each average relative power spectra, we found the maximum average relative power value (y-axis) between 20 to 100 Hz (x-axis). At frequencies below 20 Hz, the overall envelope of the inspiratory burst contributes high average relative power values (Figures 4C and D) that confound our examination of short time scale synchrony. At frequencies above 100 Hz, the average relative power values computed from XII rootlet recordings obtained using the rhythmically active slice preparation consistently diminish to baseline. For these reasons, we limited our investigation of average relative power to frequencies between 20 to 100 Hz. For each pair of average relative power spectra (control and high K^+), the greatest relative power value between 20–100 Hz was defined as the ”dominant peak”. A 10 Hz bin was centered on the frequency at which the dominant peak occurred. We computed the fraction of relative power within this 10 Hz bin. To do this, we added all points within the 10 Hz bin containing the dominant peak and divided that number by the total relative power from 0–99 Hz. By computing the fraction of relative power for each recording condition, we measured changes in the relative power of short time scale synchronous oscillations following local perfusion of high K^+. In summary,

the phrase “relative power of oscillations” refers to the average relative power in the 10 Hz bin containing the dominant peak. Changes in the relative power of oscillations are changes in the fraction of total relative power that is found in the 10 Hz bin. Paired t-tests were used to compare changes in relative power between control and elevated K^+ conditions.

Cross-correlation histograms (CCHs) of left and right XII rootlet activity were computed (Igor Pro) using the same 7–18 inspiratory bursts selected for power spectra and coherence analysis. For each pair of inspiratory bursts, the spike times in the left and right rootlet recordings were determined by amplitude discrimination as previously done for multiunit recordings acquired using the rhythmic slice preparation (Peever and Duffin,2001; Li et al.,2003). Next, the time lags between the occurrence of a given spike in the left rootlet recording and the occurrences of all spikes in the right XII rootlet recording were measured. The CCHs computed for each inspiratory burst were averaged and the y-axis of the average CCH was normalized relative to the total number of spikes in the left rootlet recording. Therefore, the y-axis reflects the probability of occurrence of a spike in each bin along the x-axis. In computing all CCHs, inspiratory motor discharge recorded from the XII rootlet ipsilateral and contralateral to local perfusion were used as the “stimulus” and “response”, respectively. For all CCHs, we set the bin width to 2 ms, which is similar to the 1 ms bin width that Sears and Stagg (1976) used in their examination of short time scale synchrony within inspiratory motor output. For each CCH, the strength of synchronization was expressed as the *k* ratio as previous done for CCHs of single and multiunit recordings acquired from respiratory neurons (Sears and Stagg,1976; Graham and Duffin,1981; Li et al.,2003). The *k* ratio is defined as the ratio of the total counts in the peak region of the CCH to the mean bin count in the region of the CCH outside of the peak (Nordstrom et al.,1992). To determine the statistical significance of the peak, we estimated the variance of the *k* ratio (σ_k^2) as: $\sigma_k^2 = k \times (\sigma_{baseline}^2/m_{baseline}^2)$, where *k* is the *k* ratio, $\sigma_{baseline}^2$ is variance of the bin count and $m_{baseline}$ is the mean bin count. The latter two were computed from the spike probability values in the region away from the peak. The peak was considered statistically significant at $p<0.05$ if $k > 1.96 \times$ the square root of σ_k^2 (Sears and Stagg,1976; Moore and McCabe,1999). The half amplitude width was computed by determining the duration of the peak in the CCH at its half amplitude. All values are expressed as means ± SE. Paired t-tests were used to compare changes in half amplitude width, time lag of peak, and total counts in the peak region between control and elevated K^+ conditions.

Coherence plots of left and right XII rootlet activity were computed to determine whether the frequency of short time scale synchronous oscillations was the same bilaterally. Each coherence plot was computed from the average absolute power spectra for the left and right rootlet recordings and the cross spectra of the two average absolute power spectra. For each coherence plot, data points were computed in 1–2 Hz intervals. By incorporating the number of inspiratory bursts used to make each coherence plot, upper 95% confidence limits were calculated using the following equation: upper 95% confidence limit = $1-(0.05)^{1/(n-1)}$ where n = # of inspiratory bursts selected for analysis. The upper 95% confidence limit is shown as a horizontal dashed line in the coherence plots (for example see Figure 7E). Coherence values above this line are significantly different from zero and are evidence for the presence of correlation between the left and right XII rootlet activity at a given frequency (Halliday and Rosenberg,2006). For each coherence plot, all coherence values from 0–99 Hz that were greater than the confidence limit were computed and summed. The resulting sum represents the significant coherence for each coherence plot. Paired t-tests were used to compare changes in the significant coherence between control and elevated K^+ conditions.

Peak integrated activity and burst duration were measured in Igor Pro using the rectified and integrated traces of the inspiratory bursts. Peak integrated activity was the measured value of the highest point of the rectified and integrated traces. Burst duration was defined as the time at 95% of the total integrated area subtracted from the time at 5% of the integrated area. Peak

integrated activity and burst duration values were computed for the same 7–18 inspiratory bursts used for power spectral analysis. The average peak integrated activity and burst duration were compared across recording conditions. Paired t-tests were used to determine statistical significance of changes in peak integrated activity, inspiratory burst duration and inspiratory burst frequency between control and elevated K^+ conditions. Following unilateral excitation of the XII nucleus, we observed an increase in peak integrated activity recorded from the ipsilateral and contralateral XII rootlet recordings. To determine whether this change in peak integrated activity was statistically different between the two sides (ipsilateral vs. contralateral), we applied a single factor analysis of variance (ANOVA).

Results

Unilateral Excitation of the PreBötC or the XII nucleus Differentially Affects Long Time Scale Synchrony

We first examined the effect of unilateral excitation of either the PreBötC or the XII nucleus on parameters of long time scale synchrony to confirm that the excitatory effect of the local perfusate was restricted to our target region. In each experiment, we recorded inspiratory-phase activity from the left and right XII rootlets while bathing the slice in ACSF containing 8mM K^+. In this recording condition, we locally and unilaterally perfused the PreBötC or the XII nucleus (Figure 1) with control ACSF (8mM K^+) containing fast green. Next, we switched the local perfusate to ACSF containing a higher concentration of K^+ and the same concentration of fast green. Fast green was included in all local perfusate solutions to monitor the spread of ACSF containing the dye and to ensure that the dye remained unilateral and localized to the PreBötC or XII nucleus.

Unilateral excitation of the PreBötC on characteristics of long time scale synchrony were quantified by computing changes in mean inspiratory burst frequency, mean peak integrated activity and mean burst duration. Although two concentrations of K^+ were locally perfused into the unilateral PreBötC, the effects of 60 and 80 mM K^+ on inspiratory activity were not different. Therefore, data from experiments using the two K^+ concentrations were pooled. For all experiments (control and high K^+) in which inspiratory activity was recorded bilaterally, each inspiratory burst in the left rootlet recording was matched by a simultaneously occurring inspiratory burst in the right rootlet recording. Unilateral excitation of the PreBötC bilaterally increased mean inspiratory burst frequency by 296 ± 66% (control: 0.09 ± 0.007 Hz versus high K^+: 0.4 ± 0.07 Hz, n=10, $p< 0.01$) (Figure 2A and B). Local perfusion of high K^+ did not significantly affect mean peak integrated activity of inspiratory bursts recorded from the ipsilateral (IPSI: 110 ± 5 % of control, n=10, n.s.) nor the contralateral (CONTRA: 110 ± 6 % of control, n = 10, n.s.) XII rootlet (Figure 2C). Unilateral excitation of the PreBötC also did not significantly affect mean inspiratory burst duration recorded from the ipsilateral (control: 527 ± 37 ms, high K^+: 532 ± 38 ms, n=10, n.s.) nor the contralateral (control: 516 ± 37 ms, high K^+: 521 ± 38 ms; n=10, n.s.) XII rootlet (Figure 2D).

Next, we investigated the effect of unilateral excitation of the XII nucleus on the characteristics of long time scale synchrony. In contrast to the effect of unilateral excitation of the PreBötC, unilateral excitation of the XII nucleus, did not significantly affect mean inspiratory burst frequency bilaterally (control: 0.1 ± 0.01 Hz versus high K^+: 0.1 ± 0.02 Hz, n=10, n.s.)(Figure 3A and B). However, local unilateral perfusion of high K^+ to the XII nucleus significantly increased mean peak integrated activity by 41 ± 10 % (n=10, $p<0.001$) in the ipsilateral rootlet recording and by 17 ± 7 % in the contralateral rootlet recording (n=10, $p<0.05$) (Figure 3A and C). Although the percent increase in peak integrated activity observed in the ipsilateral rootlet recording was greater than that measured in the contralateral rootlet recording, the effects were not statistically different from each other (single factor ANOVA, n.s.). As with unilateral PreBötC excitation (Figure 2D), unilateral excitation of the XII nucleus did not significantly

affect mean inspiratory burst duration in the ipsilateral (control: 546 ± 26 ms, high K^+: 539 ± 16 ms, n=10, n.s.) or the contralateral rootlet recording (control: 537 ± 31 ms, high K^+: 524 ± 21 ms; n=10, n.s.) (Figure 3D).

Unilateral Excitation of the XII Nucleus, but Not the PreBötC, Increases the Power of Short Time Scale Synchronous Oscillations

We investigated the effect of unilateral excitation of the PreBötC or XII nucleus on the relative power of short time scale synchronous oscillations recorded from the ipsilateral and contralateral XII rootlets. To do this, we computed average relative power spectra for inspiratory bursts recorded from the ipsilateral and contralateral XII rootlets in control conditions and following local unilateral perfusion of high K^+ to the PreBötC or XII nucleus.

Unilateral excitation of the XII increased the relative power of oscillations recorded from the ipsilateral, but not the contralateral XII rootlet (Figure 4). Representative raw filtered (1–200 Hz bandpass) inspiratory bursts recorded from the ipsilateral and contralateral XII rootlets in the control condition and following unilateral local perfusion of high K^+ onto the XII nucleus are shown in Figures 4A and B. Using the slice recordings shown in Figures 4A and B, the relative power spectra of 14 different inspiratory bursts were averaged for the left and right rootlet recordings and for each of the two conditions. The ipsilateral and contralateral average relative power spectra are shown in Figures 4C and D, respectively. In Figure 4C, the 36–46 Hz bins contain the dominant peaks for the average power spectra in control and following high K^+ application. The bin was centered around the dominant peaks at 40Hz that are present in power spectra computed for both conditions. During unilateral local perfusion of high K^+ to the XII nucleus, the fraction of relative power in the 36–46 Hz bins increased by 39%. In Figure 4D, the 10 Hz bin was centered around the dominant peak that reached the highest relative power value. Among the two average relative power spectra, the highest dominant peak occurred at 33 Hz in the power spectrum that was computed from inspiratory bursts recorded during local perfusion of high K^+ (gray). In the control power spectrum (black), there was also a peak at 47 Hz, however the relative power of this peak was less than that in the high K^+ power spectrum. Therefore for both power spectra, we computed the change in relative power in the 29–39 Hz bins that were centered around the dominant peak at 33 Hz. During unilateral local perfusion of high K^+ to the XII nucleus, the fraction of relative power in the 29–39 Hz bins increased by 29%. When we averaged the effects of unilateral excitation of the XII nucleus on oscillation power (n=7 slices), there was no statistically significant increase in the relative power of oscillations recorded from the contralateral XII rootlet (see Figure 5 and below).

Although unilateral excitation of the XII nucleus increased the relative power of short time scale synchronous oscillations recorded from the ipsilateral XII rootlet, unilateral excitation of the PreBötC had no effect on the oscillation power recorded from either the ipsilateral or contralateral XII rootlet (Figure 5). The effect of unilateral PreBötC excitation on oscillation power was examined in 7 rhythmic slices. For experiments in which high K^+ was unilaterally perfused onto the PreBötC, the effects of 60 and 80 mM K^+ on oscillation power were not different. Therefore, data from experiments using the two K^+ concentrations were pooled (n=7). Figure 5 shows that unilateral local perfusion of high K^+ to the PreBötC had no significant effect on oscillation power recorded from the ipsilateral (15 ± 13%, n.s.) and contralateral (10 ± 16%, n.s.) XII rootlet. Unilateral excitation of the XII nucleus significantly increased the relative power of oscillations (Figure 5) recorded from the ipsilateral XII rootlet (by 50 ± 17%, n=7, $p<0.05$), but had no significant effect on oscillation power recorded from the contralateral XII rootlet (21 ± 19%, n=7, n.s.). Importantly, following unilateral excitation of the XII nucleus, there was no significant correlation between the percent increase in peak integrated activity and the percent increase in the relative power of oscillations (n=7, $y = -0.2x$

+ 59, $r^2 = 0.02$, n.s.). This is supported by previous work in which we determined that there is no correlation between changes in peak integrated activity and in the relative power of oscillations (Sebe et al.,2006).

Although Bilaterally Recorded Inspiratory Motor Discharges are Crosscorrelated, Short Time Scale Synchronous Oscillations are Only Weakly Coherent

Our finding that oscillation power increases in response to unilateral excitation of the XII nucleus, and not the PreBötC, suggests that short time scale synchronous oscillations are generated at or immediately upstream of the motoneuron level. Previous studies of short time scale synchronous oscillations that are generated at the motoneuron level (termed MFOs) have shown that MFOs that are bilaterally recorded from inspiratory nerves are weakly coherent (Cohen et al.,1987; Christakos et al.,1991).

To investigate synchrony between the left and right XII rootlet discharge, we applied crosscorrelation and coherence analyses in order to assess the different forms of neural synchrony that may exist in the system. First, crosscorrelation analysis determines whether two signals are temporally correlated by measuring the time lag between, in this case, action potentials in the left and right XII rootlet recordings. A peak in the crosscorrelation plot that is centered at or near a time lag of zero provides evidence that action potentials in the left and right XII nuclei are triggered by common synaptic input (Sears and Stagg,1976; Kirkwood et al.,1982). Second, coherence analysis assesses whether the action potentials in the left and right XII rootlets share spectral characteristics. A sharp peak in the coherence plot, which is a hallmark of strong coherence, is evidence that oscillations in action potential firing that are recorded from the left and right XII rootlets occur at the same frequency (Cohen et al.,1987). It is important to keep in mind that coherence does not require synchronous activity. Neurons firing at the same frequency can produce a sharp peak in the coherence plot even if the neurons are firing out of phase and independently of each other. Therefore, crosscorrelation analysis reflects the synchrony produced by temporally correlated action potentials triggered by a common input. Coherence analysis reveals the synchrony produced when action potentials (or subthreshold changes in membrane potential) occur at the same frequency.

CCHs of left and right XII rootlet activity recorded in the control condition demonstrated that bilaterally recorded spike firing is temporally correlated. All CCHs were characterized by one of three types of peaks centered at or near a time lag of zero (Figure 6). First, 5 out of 14 control CCHs featured narrow peaks (mean half amplitude width = 6 ± 0.5 ms) centered around an average time lag of 0.4 ± 0.4 ms. Second, 4 out of 14 CCHs were characterized by broad peaks (mean half amplitude width = 23 ± 2 ms) centered around an average time lag of −2.5 ± 2.0 ms. For all CCHs displaying either narrow or broad peaks, the peaks were statistically significant ($p<0.05$). The remaining 5 out of 14 CCHs also displayed a peak in the spike probability at or near a time lag of zero (mean time lag = −0.4 ± 0.6 ms). However, the spike probability gradually decreased and a peak could not be distinguished from the baseline. For this reason, we were not able to calculate the half amplitude width for the third category of peaks. None of the CCHs displayed subsidiary harmonic peaks that arise when action potentials fire at a particular interval in a temporally correlated manner (Kirkwood et al.,1982;Christakos et al.,1991). Harmonic peaks would reflect bilaterally short time scale synchronous oscillations in spike firing that are triggered by a common synaptic input (Kirkwood et al.,1982;Christakos et al.,1991). Representative CCHs displaying either a narrow or broad peak or a peak in the spike probability that cannot be distinguished from baseline are shown in Figures 6A, B and C, respectively. All three types of CCHs in this figure exhibited a peak centered at or near a time lag of zero and lack subsidiary harmonic peaks.

Next, we determined whether there were changes in the temporal correlation of spike firing following unilateral excitation of either the XII nucleus or the PreBötC. To do this, we

computed CCHs using recordings of left and right XII rootlet activity in the control condition and following local perfusion of high K^+. For all CCHs, we obtained the time lag of the peak and the spike probability at the peak because these measures of temporal correlation could be computed regardless of the type of central peak the bilateral inspiratory discharge produced. To examine the effect of unilateral excitation of the PreBötC, we pooled the data from CCHs characterized by the three types of peaks. Unilateral high K^+ application to the PreBötC did not change the mean time lag of the peak (control: 0 ± 0.4 ms, high K^+: 0.6 ± 0.4 ms, n=7, n.s.) or the mean spike firing probability at the peak (control: 0.70 ± 0.06, high K^+: 0.72 ± 0.06 ms, n=7, n.s.). Further, high K^+ application did not introduce subsidiary harmonic peaks to the CCHs. Likewise, unilateral high K^+ application to the XII did not change the mean time lag of the peak (control: −1.4 ± 1.0 ms, high K^+: 1.7 ± 1.8 ms, n=7, n.s.) or the mean spike firing probability at the peak (control: 0.51 ± 0.05, high K^+: 0.78 ± 0.14, n=7, n.s.), and also did not introduce harmonic peaks to the CCHs.

Coherence plots were computed using the left and right average absolute power spectra for 14 pairs of XII rootlets in control conditions and following local perfusion of high K^+ (total of 28 coherence plots). Of the 28 coherence plots computed, only 3 coherence plots displayed a sharp, significant peak that reflects strong coherence (Cohen et al.,1997). The remaining 25 out of 28 plots showed only weak but significant coherence reflected by many small peaks that rose above the upper 95% confidence limit. Representative raw filtered (1–200 Hz bandpass) inspiratory bursts recorded from the ipsilateral and contralateral XII rootlets during unilateral local perfusion of high K^+ onto the XII nucleus are shown in Figures 7A and B, respectively. Using the recordings such as those shown in Figures 7A and B, the absolute power spectra of 12 different inspiratory bursts were averaged for the ipsilateral and contralateral rootlet recordings. The ipsilateral and contralateral average absolute power spectra are shown in Figures 7C and D, respectively. Dominant peaks in the ipsilateral and contralateral average absolute power spectra occur at 46 and 38 Hz (dashed vertical lines), respectively. In the corresponding coherence plot (Figure 7E), 38 and 46 Hz are marked by the two dashed vertical lines and the upper 95% confidence limit is marked by the dashed horizontal line. Coherence is not significant at either 46 or 38 Hz and the coherence plot does not exhibit strong dominant peaks. However, the bilaterally recorded XII rootlet activity is weakly coherent as demonstrated by the multiple small peaks that rise above the confidence limit between 22 and 100 Hz. The coherence plot in Figure 7E was truncated at frequencies below 22 Hz, because the overall envelopes of the inspiratory bursts produced significant coherence at these low frequencies.

For each coherence plot computed for control conditions and following unilateral local perfusion of high K^+, we measured the statistically significant coherence from 0–99 Hz. The statistically significant coherence is defined as the coherence greater than the upper 95% confidence limit (see Methods). Unilateral excitation of the PreBötC had no effect on significant coherence from 0–99 Hz (control: 10 ± 1; unilateral PreBötC excitation: 10 ± 1, n=7, n.s.). Unilateral excitation of the XII nucleus also had no effect on significant coherence from 0–99 Hz (control: 11 ± 2; unilateral XII nucleus excitation: 9 ± 1, n=7, n.s.). Therefore, neither unilateral excitation of the PreBötC nor the XII nucleus affected the coherence of oscillations recorded from the ipsilateral and contralateral XII rootlets.

Discussion

In the present work, we examined long and short time scale synchrony in the inspiratory network by applying a combination of experimental and data analysis techniques. The principal findings of this work are twofold. First, we demonstrated that unilateral excitation of the PreBötC versus the XII nucleus has differential effects on inspiratory XII nerve activity recorded bilaterally. Second, based on the results from local perfusion experiments and

crosscorrelation and coherence analyses we conclude that short time scale synchronous oscillations exhibited by the rhythmically active slice preparation are MFOs that are generated in or immediately upstream of the XII motor nucleus.

Inspiratory Motor Discharge is Bilaterally Synchronized on a Long Time Scale, but Not on a Short Time Scale

By applying crosscorrelation analysis to bilaterally recorded inspiratory activity, the present work confirms previous work that left and right XII rootlet discharges are temporally correlated on a long time scale (Smith et al.,1991; Funk et al.,1993). However, the absence of subsidiary harmonic peaks in the CCHs and the lack of strong coherence in the majority of the coherence plots demonstrate that inspiratory-phase short time scale synchronous oscillations recorded from the left and right XII rootlets are not temporally correlated and do not occur at the same frequency, respectively. As such, short time scale synchronous oscillations recorded from XII rootlets in the slice are MFOs that are likely generated at or immediately upstream of the XII nucleus.

Each CCH of left and right XII rootlet discharge was characterized by a narrow, broad, or very broad peak centered at or near a time lag of zero. Previously reported CCHs computed using in vivo recordings of inspiratory nerve filaments featured central peaks with similar widths and shapes (Kirkwood et al.,1982). A few hypotheses have been presented to explain the varying widths of the central peaks (Kirkwood et al.,1982). According to one of these hypotheses, the axon of a common input cell branches and innervates individual inspiratory motoneurons. Through these axonal branches, a common input cell is able to innervate, depolarize and synchronize spike firing in different inspiratory motoneurons (Sears and Stagg, 1976). If the common input cell directly innervates the motoneurons, the spike firing of individual motoneurons is precisely synchronized and this yields a narrow central peak in the CCH. Alternatively, the common input cell may trigger motoneuron firing via a combination of monosynaptic and polysynaptic circuits. Although the axonal branches of the common input cell are depolarized at the same time, the electrical signal may pass through one, two or multiple synapses before it reaches the respective motoneurons. As a result, the motoneurons receive suprathreshold synaptic inputs at different times. A motoneuron that receives suprathreshold synaptic input directly from the common input cell will fire sooner than a neighboring motoneuron for which the common input cell is two or more synapses away. Therefore, if the common input cells and the motoneurons are linked by combination of monosynaptic and polysynaptic circuits the time lag between spikes recorded from the left and right XII rootlet will vary. Depending on which circuits are more intact in the slice, the time lags will yield a narrow or broad central peak.

From retrograde viral tracing studies, we know that premotoneurons send projections to the ipsilateral and contralateral XII nucleus (Dobbins and Feldman,1995; Chamberlin et al., 2007). Although the left and right PreBötCs project to and synchronize each other (Koshiya and Smith,1999), there is no evidence that PreBötC neurons project either unilaterally or bilaterally to the XII nucleus. Therefore, it is possible that HM spike firing is bilaterally synchronized on a long time scale via bilaterally projecting axonal branches of premotoneurons. Further, premotoneurons and HMs may be connected via a combination of monosynaptic and polysynaptic circuitry.

Although spike firing between the left and right XII rootlet recordings are temporally correlated on a long time scale, the CCHs and coherence plots presented here provide strong evidence that inspiratory motor discharge recorded *in vitro* is not bilaterally synchronized on a short time scale. If action potentials in the bilateral XII rootlet activity were temporally correlated and occur within the same frequency range, the central peak in each CCH would be flanked by subsidiary harmonic peaks and the cycle time of each harmonic peak would correspond to

the cycle time of a single synchronous oscillation (Kirkwood et al.,1982; Cohen et al.,1987; Christakos et al.,1991). Such harmonic peaks are characteristic of CCHs computed from neural activity exhibiting HFOs that are generated and synchronized via a common input source. None of the CCHs computed in this study exhibit harmonic peaks. This suggests that short time scale synchronous oscillations recorded from the left and right XII rootlets *in vitro* are MFOs.

This conclusion is further supported by the results of coherence analysis. If the bilateral rootlet recordings exhibited short time scale oscillations occurring at the same frequency but were not necessarily temporally coincident, then the coherence plots should display a prominent and significant peak, which is characteristic of HFOs. We found that the vast majority of coherence plots (25 out of 28) showed only small peaks rising above the 95% confidence limit. This is consistent with previous work in the decerebrate cat that found based on bilateral hypoglossal nerve recordings that coherence peaks were “appreciable” in the HFO range but “rare” in the MFO range (Cohen et al.,1987).

The presence of a central peak and the absence of harmonic peaks in all CCHs in addition to the lack of prominent peaks in almost all of the coherence plots support our conclusion that inspiratory XII rootlet discharge is bilaterally synchronized on a long time scale but not on a short time scale. Given that oscillations recorded from the left and right XII rootlets are not bilaterally temporally coincident and do not occur at the same frequency, they can be categorized as MFOs (Cohen et al.,1987; Christakos et al.,1991) and are likely generated in or immediately upstream of the XII nucleus.

Origin of Short Time Scale Synchronous Oscillations in the Rhythmic Slice

The principal aim of the present study was to determine where in the rhythmically active slice preparation short time scale synchronous oscillations are generated. Together, the data from local application experiments, crosscorrelation and coherence analyses demonstrate that synchronous oscillations in the slice are MFOs that are generated in the XII nucleus or immediately upstream of the XII nucleus in the premotor area. Upon consideration of the cellular architecture that is required to generate short time scale synchronous oscillations, we conclude that such oscillations are likely generated in the premotor area and not in the XII nucleus. Our conclusion is limited to short time scale synchronous oscillations recorded from the rhythmically active slice preparation and does not necessarily apply to oscillations studied in more intact preparations such as the brainstem-spinal cord preparation.

The PreBötC is thought to propagate inspiratory rhythm to multiple motor pools, including the XII nucleus, via premotoneurons that are located in an intermediate zone between the PreBötC and the motor nuclei (Dobbins and Feldman,1995; Luo et al.,2006; Chamberlin et al.,2007). Premotoneurons that project to the HMs are located lateral and ventrolateral to the hypoglossal nucleus (Dobbins and Feldman,1995) and some of these premotoneurons are GABAergic and glycinergic (Li et al.,1997). A premotor origin for synchronous oscillations is consistent with the increase in relative power produced by excitation of the XII nucleus. If oscillations are generated in the premotor area, HMs would receive oscillatory synaptic inputs from premotoneurons. Depolarizing the resting membrane potential of HMs, by locally perfusing high K^+ onto the XII nucleus, would increase their probability of firing action potentials at the peaks of such oscillatory inputs and thereby increase the computed oscillation power. Alternatively, but not necessarily exclusively, local perfusion of high K^+ to the XII nucleus could depolarize excitatory synaptic terminals and thereby enhance the oscillatory premotor drive received by HMs.

Although the increase in relative power following unilateral excitation of the XII nucleus can be explained by a motor origin for synchronous oscillations, neurons in the XII nucleus lack the cellular morphology and synaptic properties necessary to generate synchronous

oscillations. In previous work from our laboratory, we demonstrated that GABAergic and glycinergic transmission are required to generate short time scale synchronous oscillations (Bou-Flores and Berger,2001; Sebe et al.,2006). Further, studies in the hippocampus (Cobb et al.,1995; Fisahn et al.,1998) and olfactory bulb (Schoppa,2006) have proposed models for the generation of synchronous oscillations. In these models, the peaks and troughs of synchronous oscillations are generated by alternating excitatory and inhibitory synaptic inputs, respectively, that are connected via recurrent axon collaterals. The XII nucleus is ill-equipped to generate short time scale synchronous oscillations because HMs lack recurrent axon collaterals and interneurons within the XII nucleus that could provide inhibitory synaptic inputs are scarce (Viana et al.,1990). Therefore, oscillations are more likely generated in the premotor area, which contains both excitatory and inhibitory neurons (Li et al.,1997), these oscillations would be transmitted to the XII nucleus.

Despite the potential importance of premotoneurons in generating short time scale synchronous oscillations, transmitting inspiratory activity to inspiratory motoneurons and in modulating inspiratory rhythm, relatively little is known about this region. In the future, it will be interesting to identify the location of the premotor area in the slice preparation and to characterize the properties of premotoneurons. This information will have important implications with respect to understanding how inspiratory rhythm is transmitted and modulated before it reaches the XII nucleus, and possibly how short time scale synchronous oscillations are generated in the premotor area.

Acknowledgements

We would like to thank Dr. J.F. van Brederode for helpful comments on the manuscript and suggestions with regard to the experimental methodology. We appreciate Dr. W. Satterthwaite's technical assistance and the help of Drs. R.K. Powers and J.A. Detwiler in recommending and writing data analysis routines. We would also like to thank Drs. J.M. Ramirez, M.A. Parkis, and G.D. Funk for technical advice. This research was supported by NIH grant HL-49657.

Abbreviations

ANOVA
: analysis of variance

ACSF
: artificial cerebrospinal fluid

CONTRA
: contralateral

CCHs
: cross-correlation histograms

HFO
: high frequency oscillation

XII
: hypoglossal

HMs
: hypoglossal motoneurons

IPSI
: ipsilateral

MFO

medium frequency oscillation

PreBötC

PreBötzinger Complex

References

Baker MR, Baker SN. The effect of diazepam on motor cortical oscillations and corticomuscular coherence studied in man. J Physiol 2003;546:931–942. [PubMed: 12563016]

Baker SN, Kilner JM, Pinches EM, Lemon RN. The role of synchrony and oscillations in the motor output. Exp Brain Res 1999;128:109–117. [PubMed: 10473748]

Bou-Flores C, Berger AJ. Gap junctions and inhibitory synapses modulate inspiratory motoneuron synchronization. J Neurophysiol 2001;85:1543–1551. [PubMed: 11287478]

Chamberlin NL, Eikermann M, Fassbender P, White DP, Malhotra A. Genioglossus premotoneurons and the negative pressure reflex in rats. J Physiol 2007;579:515–526. [PubMed: 17185342]

Christakos CN, Cohen MI, Barnhardt R, Shaw CF. Fast rhythms in phrenic motoneuron and nerve discharges. J Neurophysiol 1991;66:674–687. [PubMed: 1753279]

Cobb SR, Buhl EH, Halasy K, Paulsen O, Somogyi P. Synchronization of neuronal activity in hippocampus by individual GABAergic interneurons. Nature 1995;378:75–78. [PubMed: 7477292]

Cohen MI. Synchronization of discharge, spontaneous and evoked, between inspiratory neurons. Acta Neurobiol Exp (Wars) 1973;33:189–218. [PubMed: 4698501]

Cohen, MI.; Huang, W.; See, WR.; Yu, Q.; Christakos, CN. Fast Rhythms in Respiratory Neural Activities. In: Miller, AD.; Bianchi, AL.; Bishop, BP., editors. Neural Control of Respiratory Muscles. Boca Raton: CRC Press; 1997. p. 159-169.

Cohen MI, See WR, Christakos CN, Sica AL. High-frequency and medium-frequency components of different inspiratory nerve discharges and their modification by various inputs. Brain Res 1987;417:148–152. [PubMed: 3113671]

Dobbins EG, Feldman JL. Differential innervation of protruder and retractor muscles of the tongue in rat. J Comp Neurol 1995;357:376–394. [PubMed: 7673474]

Fisahn A, Pike FG, Buhl EH, Paulsen O. Cholinergic induction of network oscillations at 40 Hz in the hippocampus in vitro. Nature 1998;394:186–189. [PubMed: 9671302]

Funk GD, Parkis MA. High frequency oscillations in respiratory networks: functionally significant or phenomenological? Respir Physiol Neurobiol 2002;131:101–120. [PubMed: 12106999]

Funk GD, Smith JC, Feldman JL. Generation and transmission of respiratory oscillations in medullary slices: role of excitatory amino acids. J Neurophysiol 1993;70:1497–1515. [PubMed: 8283211]

Gelperin A. Olfactory computations and network oscillation. J Neurosci 2006;26:1663–1668. [PubMed: 16467512]

Graham K, Duffin J. Cross correlation of medullary expiratory neurons in the cat. Exp Neurol 1981;73:451–464. [PubMed: 7021170]

Halliday, DM.; Rosenberg, JR. Time and Frequency Domain Analysis of Spike Train and Time Series Data. In: Windhorst, U.; Johansson, H., editors. Modern Techniques in Neuroscience Research. Berlin: Springer; 2006. p. 503-543.

Johnson SM, Koshiya N, Smith JC. Isolation of the kernel for respiratory rhythm generation in a novel preparation: the pre-Botzinger complex “island”. J Neurophysiol 2001;85:1772–1776. [PubMed: 11287498]

Kahana MJ. The cognitive correlates of human brain oscillations. J Neurosci 2006;26:1669–1672. [PubMed: 16467513]

Kirkwood PA, Sears TA, Tuck DL, Westgaard RH. Variations in the time course of the synchronization of intercostal motoneurones in the cat. J Physiol 1982;327:105–135. [PubMed: 7120134]

Koshiya N, Guyenet PG. Tonic sympathetic chemoreflex after blockade of respiratory rhythmogenesis in the rat. J Physiol 1996;491(Pt 3):859–869. [PubMed: 8815217]

Koshiya N, Smith JC. Neuronal pacemaker for breathing visualized in vitro. Nature 1999;400:360–363. [PubMed: 10432113]

Li YM, Shen L, Peever JH, Duffin J. Connections between respiratory neurones in the neonatal rat transverse medullary slice studied with cross-correlation. J Physiol 2003;549:327–332. [PubMed: 12692183]

Li YQ, Takada M, Kaneko T, Mizuno N. Distribution of GABAergic and glycinergic premotor neurons projecting to the facial and hypoglossal nuclei in the rat. J Comp Neurol 1997;378:283–294. [PubMed: 9120066]

Luo P, Zhang J, Yang R, Pendlebury W. Neuronal circuitry and synaptic organization of trigeminal proprioceptive afferents mediating tongue movement and jaw-tongue coordination via hypoglossal premotor neurons. Eur J Neurosci 2006;23:3269–3283. [PubMed: 16820017]

Moore, DS.; McCabe, GP. Introduction to the Practice of Statistics. New York: W.H. Freeman and Company; 1999. Introduction to Inference; p. 433-501.

Nordstrom MA, Fuglevand AJ, Enoka RM. Estimating the strength of common input to human motoneurons from the cross-correlogram. J Physiol 1992;453:547–574. [PubMed: 1464844]

Parkis MA, Feldman JL, Robinson DM, Funk GD. Oscillations in endogenous inputs to neurons affect excitability and signal processing. J Neurosci 2003;23:8152–8158. [PubMed: 12954878]

Peever JH, Duffin J. Bilateral synchronisation of respiratory motor output in rats: adult versus neonatal in vitro preparations. Pflugers Arch 2001;442:943–951. [PubMed: 11680628]

Pierrefiche O, Schwarzacher SW, Bischoff AM, Richter DW. Blockade of synaptic inhibition within the pre-Botzinger complex in the cat suppresses respiratory rhythm generation in vivo. J Physiol 1998;509(Pt 1):245–254. [PubMed: 9547397]

Richardson CA, Mitchell RA. Power spectral analysis of inspiratory nerve activity in the decerebrate cat. Brain Res 1982;233:317–336. [PubMed: 6800563]

Schoppa NE. Synchronization of olfactory bulb mitral cells by precisely timed inhibitory inputs. Neuron 2006;49:271–283. [PubMed: 16423700]

Seager MA, Johnson LD, Chabot ES, Asaka Y, Berry SD. Oscillatory brain states and learning: Impact of hippocampal theta-contingent training. Proc Natl Acad Sci U S A 2002;99:1616–1620. [PubMed: 11818559]

Sears TA, Stagg D. Short-term synchronization of intercostal motoneurone activity. J Physiol 1976;263:357–381. [PubMed: 1018273]

Sebe JY, van Brederode JF, Berger AJ. Inhibitory synaptic transmission governs inspiratory motoneuron synchronization. J Neurophysiol 2006;96:391–403. [PubMed: 16510772]

Smith JC, Ellenberger HH, Ballanyi K, Richter DW, Feldman JL. Pre-Botzinger complex: a brainstem region that may generate respiratory rhythm in mammals. Science 1991;254:726–729. [PubMed: 1683005]

Steriade M, McCormick DA, Sejnowski TJ. Thalamocortical oscillations in the sleeping and aroused brain. Science 1993;262:679–685. [PubMed: 8235588]

Stopfer M, Bhagavan S, Smith BH, Laurent G. Impaired odour discrimination on desynchronization of odour-encoding neural assemblies. Nature 1997;390:70–74. [PubMed: 9363891]

Viana F, Gibbs L, Berger AJ. Double- and triple-labeling of functionally characterized central neurons projecting to peripheral targets studied in vitro. Neuroscience 1990;38:829–841. [PubMed: 1702883]

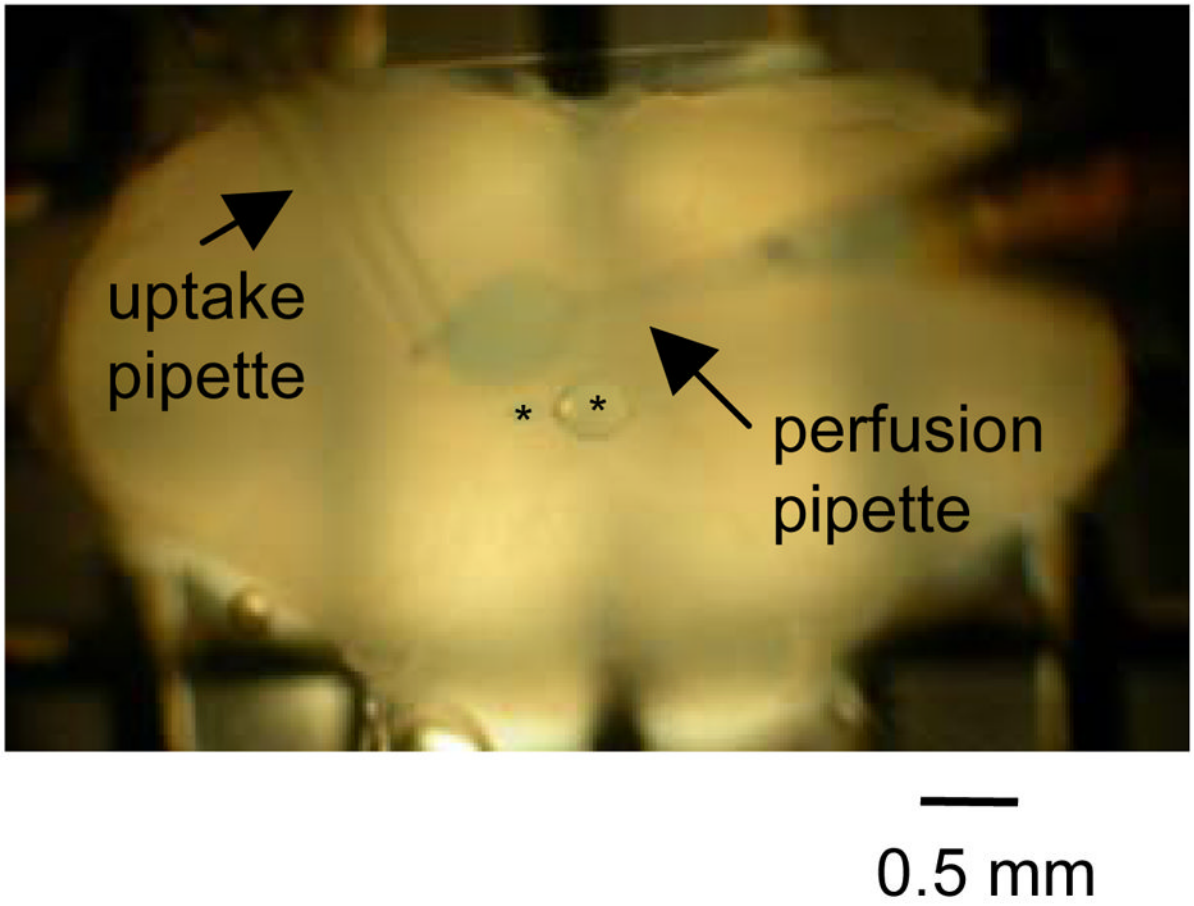

Figure 1.
Image of local unilateral perfusion. In this example, ACSF containing fast green was locally and unilaterally perfused onto the XII nucleus of a rhythmically active medullary slice preparation. Perfusion region is circumscribed to a zone approximately 0.5 mm in diameter as revealed by fast green labeled region over the left XII nucleus. Asterisks are over epoxy beads on a nylon thread that help to limit the labeled perfusion region. Arrows indicate the local perfusion pipette and the local uptake pipette.

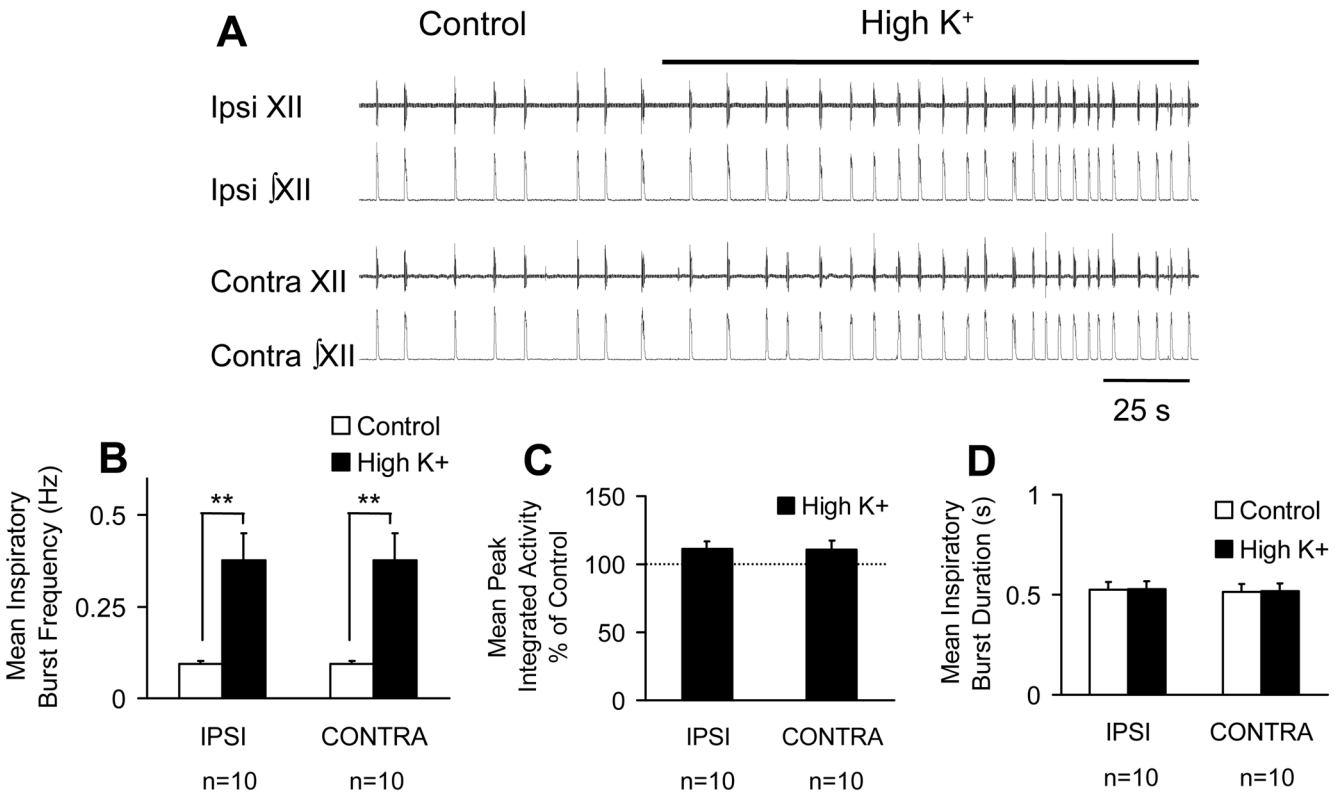

Figure 2.

Local unilateral perfusion of high K^+ to the PBC bilaterally increases inspiratory burst frequency but not peak integrated activity or inspiratory burst duration. A. Representive raw (XII) and rectified and integrated (∫XII) hypoglossal rootlet recordings from the ipsilateral (Ipsi) and contralateral (Contra) hypoglossal rootlets in the control condition and following local unilateral perfusion of high K^+ (80 mM). A and B. Local perfusion of high K^+ to the unilateral PBC bilaterally increases inspiratory burst frequency. C and D. Unilateral excitation of PBC did not significantly affect peak integrated activity or inspiratory burst duration bilaterally. $^{**}P < 0.01$; paired *t*-test v.s. control

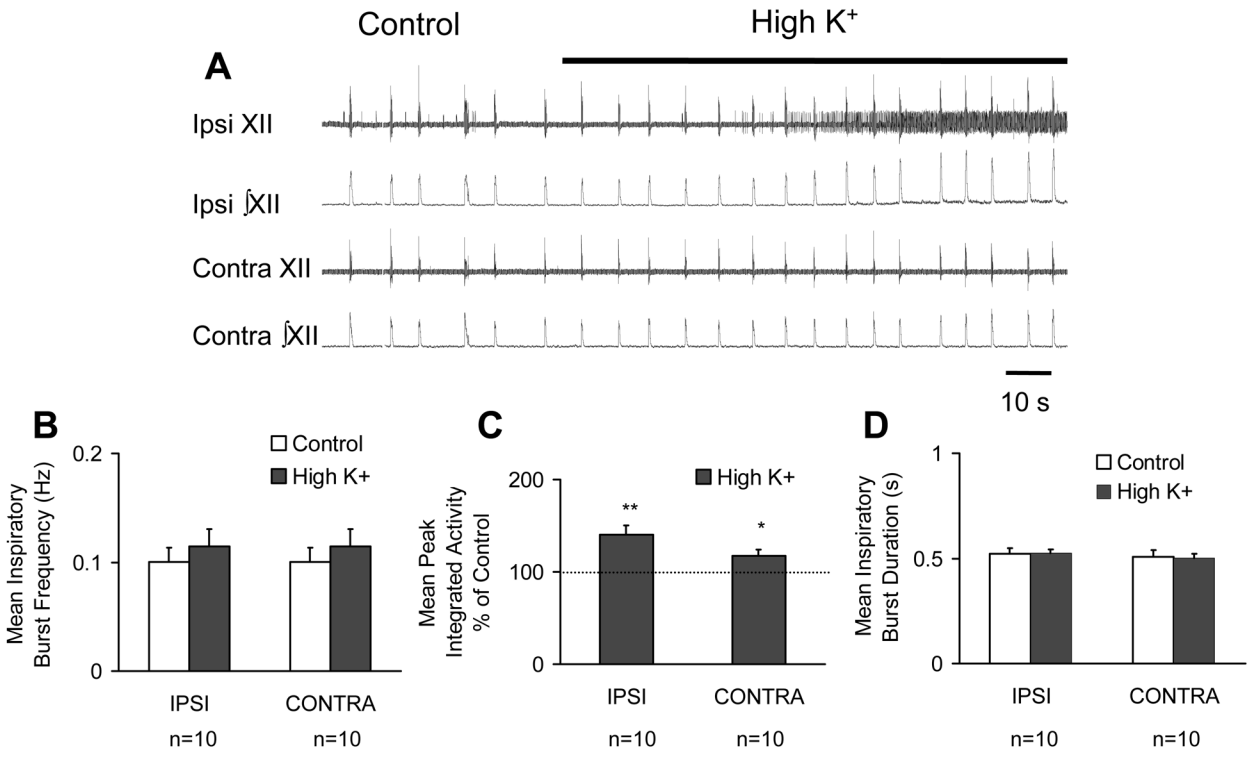

Figure 3.

Local unilateral perfusion of high K^+ to the XII nucleus bilaterally increases peak integrated activity but not inspiratory burst frequency or inspiratory burst duration. A. Representive raw (XII) and rectified and integrated (∫XII) hypoglossal rootlet recordings from the Ipsi and Contra hypoglossal rootlets in the control condition and following local unilateral perfusion of high K^+ (20 mM). A and B. Local perfusion of high K^+ to the unilateral XII nucleus did not significantly affect inspiratory burst frequency measured bilaterally. C. Unilateral excitation of the XII nucleus increased peak integrated activity in the IPSI rootlet and, to a lesser extent, in the CONTRA rootlet. D. There was no significant effect on mean inspiratory burst duration measured bilaterally. *$P < 0.05$; **$P < 0.01$; paired *t*-test v.s. control

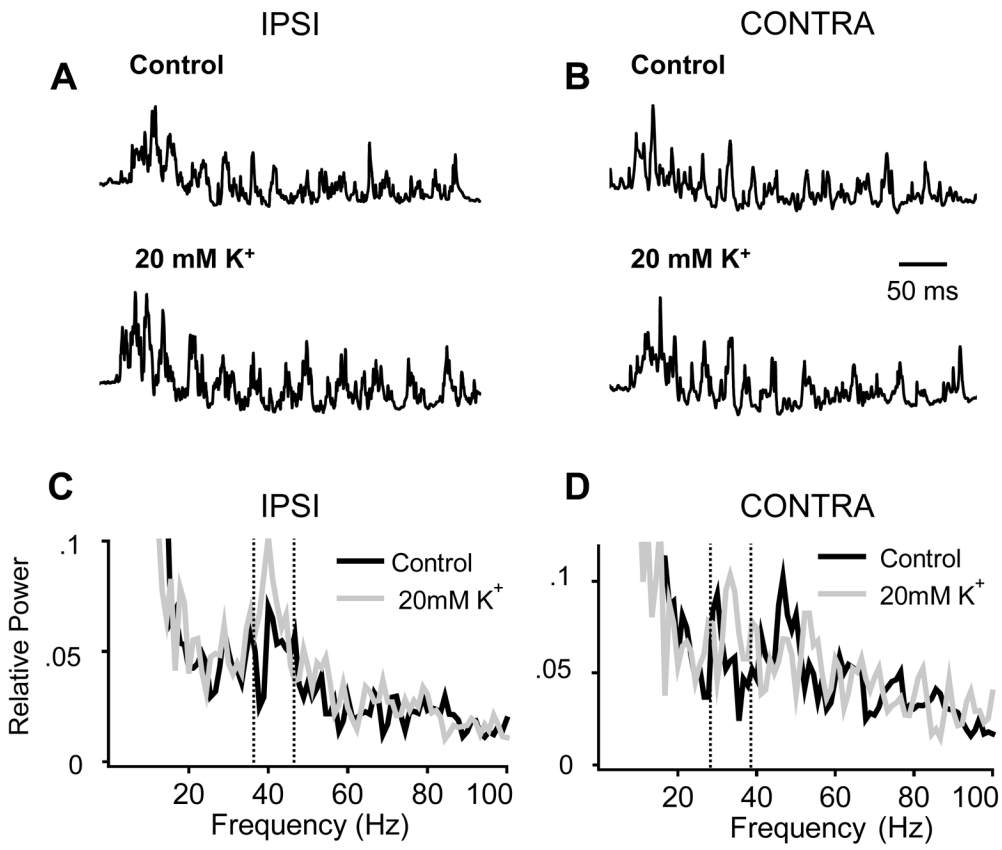

Figure 4.

High K^+ increases oscillation power when unilaterally applied to the XII nucleus. A and B. Representative raw filtered (1–200 Hz bandpass) inspiratory bursts recorded from the IPSI (A) and CONTRA (B) XII rootlet. The top traces are inspiratory bursts recorded in the control condition. The bottom traces are inspiratory bursts recorded following local perfusion of 20 mM K^+ to the IPSI XII nucleus. Same time scale applies to all inspiratory bursts. C. Ipsilateral average relative power spectra in the control condition and following local perfusion of 20 mM K^+ to the IPSI XII nucleus. Unilateral excitation of the XII nucleus increases oscillation power within the bin containing the dominant peak (36–46 Hz). D. Contralateral average relative power spectra in the control condition and following local perfusion of 20 mM K^+ to the CONTRA XII nucleus. Unilateral excitation of the XII nucleus increases oscillation power within the bin containing the dominant peak (29–39 Hz). When we averaged data for the overall population of experiments in which the XII nucleus was unilaterally excited, this increase in oscillation power was not statistically significant. The bins containing the dominant peak are marked by vertical dotted lines in the IPSI and CONTRA average relative power spectra.

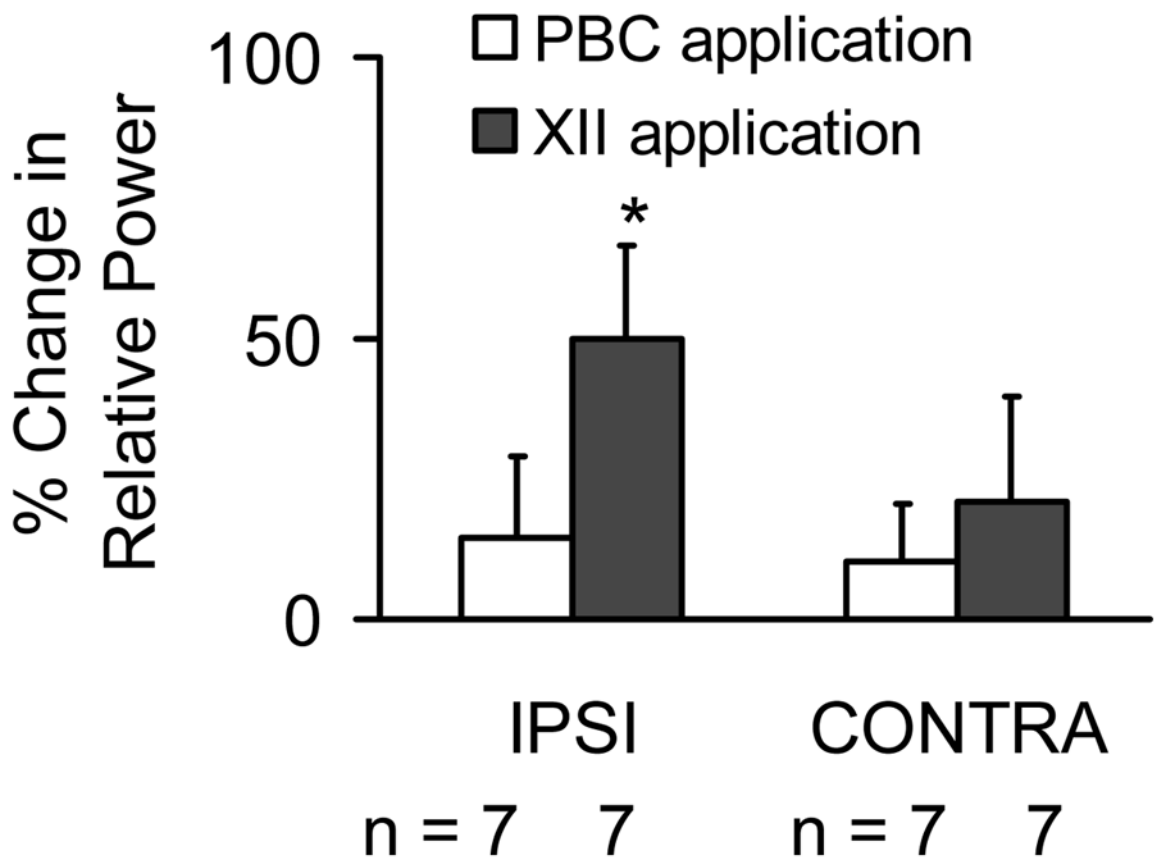

Figure 5.
Summary of the effects of unilateral excitation of the PBC or the XII nucleus on the relative power of oscillations. Local perfusion of ACSF containing high K^+ (60 or 80 mM) to the unilateral PBC had no signifiicant effect on oscillation power bilaterally. Local perfusion of ACSF containing high K^+ (20 mM) to the unilateral XII nucleus increased oscillation power in the IPSI, but had no significant effect on the oscillation power recorded from the CONTRA XII rootlet.

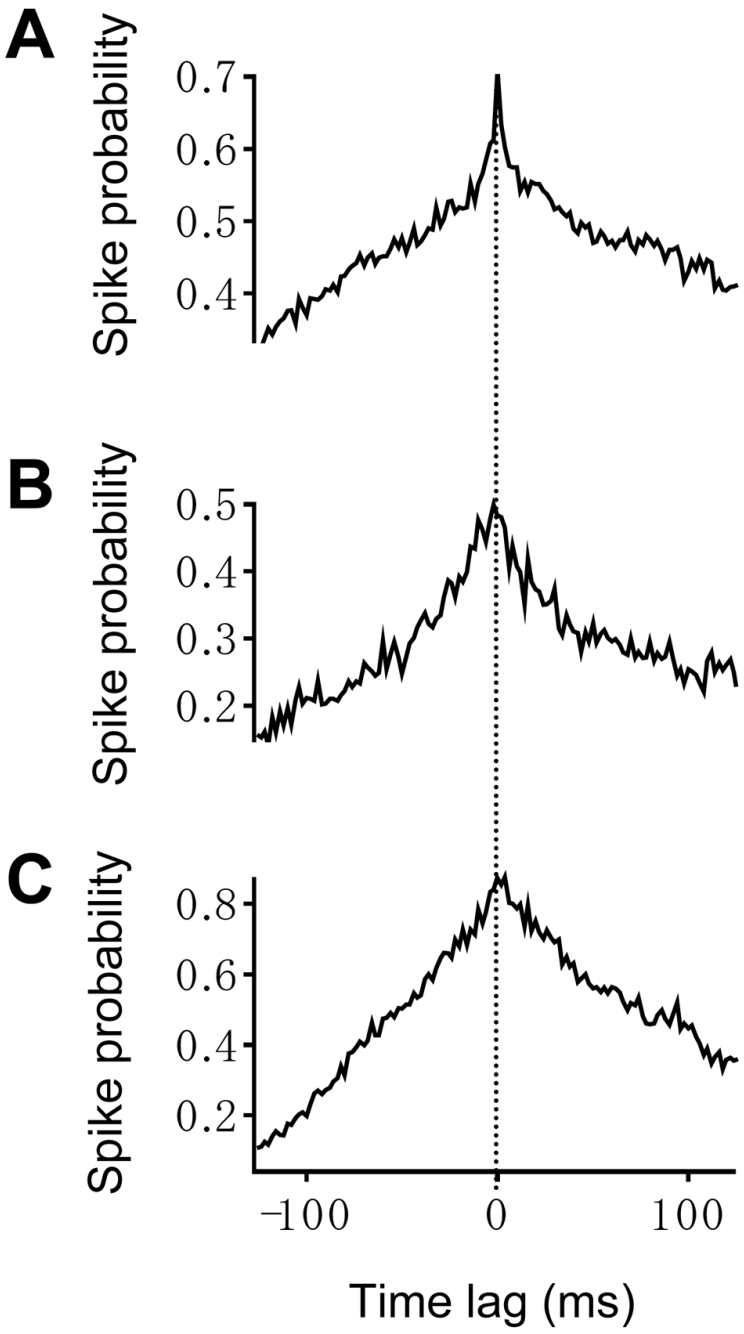

Figure 6.

Crosscorrelation histograms (CCHs) of left and right hypoglossal rootlet activity produce three types of peaks. Those three types of peaks are (1) narrow and (2) broad central peaks and (3) a peak in the spike probability that gradually decreases and is not distinguishable from the baseline spike probability. The representative CCH in (A) displays a narrow peak that occurs at a time lag of 0 ms and has a half-width of 6 ms. The representative CCH in (B) displays a broad peak that occurs at a time lag of −2 ms and has a half-width of 22 ms. The representative CCH in (C) displays a peak that occurs at a time lag of 4 ms and is not distinguishable from the baseline. None of the CCHs exhibit harmonic peaks. For all CCHs, the bin width equals 2 ms. Dashed vertical line marks zero time lag.

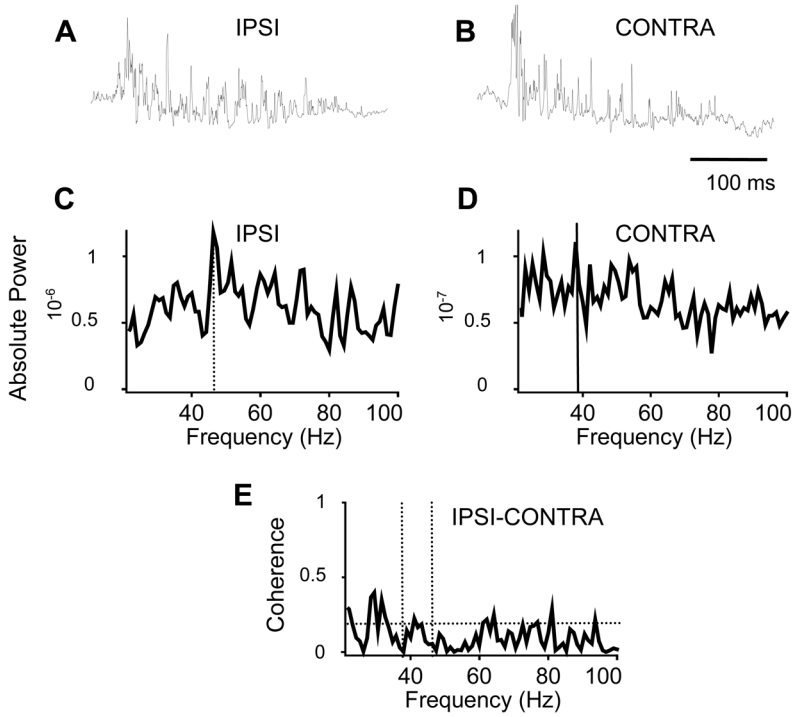

Figure 7.

Bilaterally recorded XII rootlet activity is weakly coherent. A and B. Representative raw filtered (1–200 Hz bandpass) inspiratory bursts recorded from the IPSI (A) and CONTRA (B) XII rootlet following unilateral excitation of the XII nucleus. C and D. IPSI and CONTRA average absolute power spectra each computed from 12 inspiratory bursts recorded following unilateral excitation of the XII nucleus. Dashed vertical lines mark the location of the dominant peaks in the IPSI and CONTRA power spectra at 46 and 38 Hz, respectively. E. Coherence plot computed from the IPSI and CONTRA average absolute power spectra in C and D. The dashed horizontal line marks the upper 95% confidence limit at 0.19. 46 and 38 Hz are marked by the dashed vertical lines. Although there are peaks in the IPSI (C) and CONTRA (D) average absolute power spectra at 46 and 38 Hz, respectively, the oscillations are not coherent at these frequencies. However, the small peaks that rise above the confidence limit between 22–100 Hz demonstrate that the left and right XII rootlet discharges are weakly coherent.